

Modeling the tunability of the dual-feedback genetic oscillatorYash J. Joshi, Yash K. Jawale[✉], and Chaitanya A. Athale^{✉*}*Division of Biology, IISER Pune, Dr. Homi Bhabha Road, Pashan, Pune 411008, India*

(Received 20 May 2019; revised manuscript received 10 October 2019; published 29 January 2020)

Oscillatory gene circuits are ubiquitous to biology and are involved in fundamental processes of cell cycle, circadian rhythms, and developmental systems. The synthesis of small, non-natural oscillatory genetic circuits has been increasingly used to test the fundamental principles of genetic network dynamics. While the “repressilator” was used to first demonstrate the proof of principle, a more recently developed dual-feedback, fast, tunable genetic oscillator has demonstrated a greater degree of robustness and control over oscillatory behavior by combining positive- and negative-feedback loops. This oscillator, combining *lacI* (negative-) and *araC* (positive-) feedback loops, was, however, modeled using multiple layers of differential equations to capture the molecular complexity of regulation, in order to explain the experimentally measured oscillations. In the search for design principles of such minimal oscillatory circuits, we have developed a reduced model of this dual-feedback loop oscillator consisting of just six differential equations, two of which are delay differential equations. The delay term is optimized, as the only free parameter, to fit the experimental dynamics of the oscillator period and amplitude tunability by the two inducers isopropyl β -D-1-thiogalactopyranoside (IPTG) and arabinose. We proceed to use our reduced and experimentally validated model to redesign the network by comparing the effect of asymmetry in gene expression at the level of (a) DNA copy numbers and the rates of (b) mRNA translation and (c) degradation, since experimental and theoretical work had predicted a need for an asymmetry in the copy numbers of activator (*araC*) and repressor (*lacI*) genes encoded on plasmids. We confirm that the minimal period of the oscillator is sensitive to DNA copy number asymmetry, and can demonstrate that while the asymmetry in the translation rate has an identical effect as the plasmid copy numbers, modulating the asymmetry in mRNA degradation can improve the tunability of the period and amplitude of the oscillator. Thus, our model predicts control at the level of translation can be used to redesign such networks, for improved tunability, while at the same time making the network robust to replication “noise” and the effects of the host cell cycle. Thus, our model predicts experimentally testable principles to redesign a potentially more robust oscillatory genetic network.

DOI: [10.1103/PhysRevE.101.012417](https://doi.org/10.1103/PhysRevE.101.012417)**I. INTRODUCTION**

The ubiquity of oscillatory genetic networks suggests a central role in biology, resulting in extensive experimental and theoretical studies as seen in the case of cell cycle clocks [1–5], circadian rhythms [6,7], and developmental clocks in embryogenesis [8–10]. These oscillatory networks appear to have been selected for tunability and robustness as a part of the general “homeostatic” mechanisms of such physiological processes critical to living systems. However, understanding the design principles of such networks raises challenges due to their complexity. Increasingly, the synthetic biology of small genetic networks has become an important alternative approach to gaining a fundamental understanding of the principles of gene regulation driving such oscillators using small and relatively tractable genetic networks, such as single gene negative-feedback systems [11], the three-component “repressilator” [12], and cell-free two- and three-stage gene cascades [13]. Based on theoretical studies of naturally occurring genetic oscillators, they have been broadly

classified into either negative-feedback loops or coupled positive and negative loops [5]. Indeed, comparative modeling has demonstrated that while a minimal negative-feedback loop network can produce oscillations, robustness and tunability are improved by the addition of a positive-feedback loop, which could explain the evolutionary selection of increasingly complex networks [14].

A canonical example of a synthetic dual-feedback loop—positive and negative—oscillator that has rapidly become a standard model is the *araC* and *lacI* genetic oscillator with expression determined by a dual input $p_{lac/ara-1}$ promoter [15]. The genes are regulated by their own protein products (feedback)—activation by the AraC protein in the presence of arabinose (positive feedback) and repression by the LacI protein in the absence of isopropyl β -D-1-thiogalactopyranoside (IPTG) (negative feedback). A model with 27 coupled ordinary differential equations (ODEs) was developed to match the experimental findings [15], since a simple minimal model of dual-feedback loops by the same authors had previously failed to reproduce the oscillatory response of the system to parameter changes [16]. The many intermediate reactions in the model, such as the relatively slower rate of mRNA production, protein folding, protein

*cathale@iiserpune.ac.in

multimerization, and promoter binding, play an important role in the experimental validation of this model. While explicit models of detailed molecular mechanisms are physically more realistic than minimal models, they also lead to an “explosion” in the number of parameters and variables. One solution is to use delay differential equations as seen for the *lac* operon [17], to simplify the model in a manner that captures the essential nature of the process, while reproducing the measurable dynamics of the system.

In the search for the general design principles of genetic oscillators, alongside topology, delays and “noise” have also been seen to play an important role, with noise acting either constructively or destructively [18]. The explicit use of delay differential equations for modeling genetic networks is seen in oscillator models of the cell cycle [5] and somitogenesis clock [9] and lac operon dynamics [17]. Indeed, a cell-free extract-based study of the lac-ara dual-feedback oscillator has demonstrated that protein translation can serve as a bottleneck in the dynamics of the oscillator [13]. The separation of timescales seen in experiment and the utility of delays in oscillatory network models together suggest that such an approach could help reduce the model complexity of the lac-ara oscillator.

Here, we describe a reduced model of the lactose-arabinose dual-feedback loop oscillator, that was first developed by Stricker *et al.* [15]. Our model consists of a system of six differential equations (DDEs), that take into account the canonical components of gene expression: DNA promoter states, RNA expression, and protein translation and stability. We introduce two delay terms, in order to account for the time taken by the intermediate states eliminated in the simplification, and fit them to the experimental dynamics reported for the oscillatory behavior. We then use this validated, simplified model to test the role of DNA copy number asymmetry of the positive- and negative-feedback loops, based on the original design of the circuit. We use this model to test whether varying the asymmetry between the ribosome binding site (RBS) efficiency of the activator and repressor would affect the behavior of the oscillator in the same way as controlling the plasmid copy number ratios. We explore experimentally testable approaches to improving the tunability of the oscillator by varying the mRNA degradation rates. Our simplified, experimentally validated model therefore enables us to improve our understanding of the network, and allows us to test potential approaches to rationally redesign the network.

II. MODEL

We have modeled the oscillator based on the coupled dynamics of (a) DNA transcription to RNA based on promoter state dynamics, (b) translation of RNA to protein, and (c) protein folding (Fig. 1).

A. Model derivation

We have derived the model equations by simplifying the detailed reaction kinetics of (a) promoter dynamics determined by protein binding, (b) RNA transcription, (c) trans-

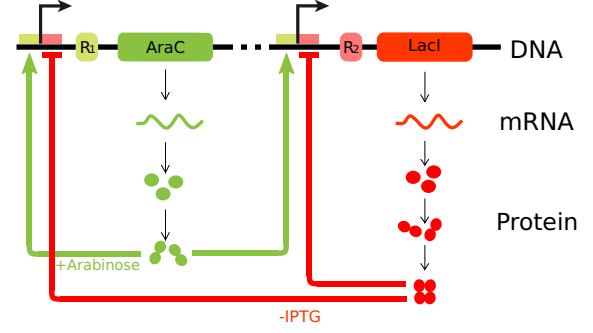
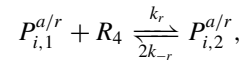
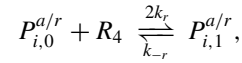
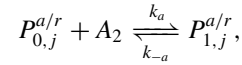


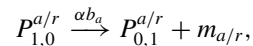
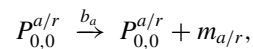
FIG. 1. Model of the *lacI-araC* tunable genetic oscillator. The schematic represents a kinetic model of the transcriptional regulation of gene expression of *araC* (green/light-gray) and *lacI* (red/dark-gray) genes by a dual-feedback loop of activation (arrowhead) by dimers of AraC proteins (green/light-gray circles) and repression (bar end) by tetramers of LacI proteins (red/dark-gray circles). The model explicitly includes mRNA transcription, protein translation, and folding and modulation of gene expression by arabinose and IPTG.

lation of mRNA, and (d) protein folding and (e) protein multimerization based on the previous work by Stricker *et al.* [15], with modifications aimed at reducing the complexity of the model. The promoter reactions in the *araC-lacI* oscillatory system are as follows,



where A_2 represents AraC protein dimers, R_4 represents LacI protein tetramers, respectively, $P_{i,j}^{a/r}$ represent the states of promoters on the activator/repressor plasmids with $i \in (0, 1)$ number of AraC dimers (A_2) bound and $j \in (0, 1, 2)$ the number of LacI tetramers (R_4) bound, and k_r and k_a are the forward and k_{-r} and k_{-a} and backward rates of A_2 and R_4 binding to the promoters, as has been described before. However, we further simplify this by assuming that the protein binding to the promoters is in equilibrium. Thus we can express the reactions in terms of equilibrium constants, the ratio of forward and backward rates, as $k_1 = k_a/k_{-a}$, $k'_2 = 2k_r/k_{-r}$, and $k''_2 = k_r/2k_{-r}$. By substituting $k_r/k_{-r} = k_2$, the equilibrium constants of the repressor binding reactions are $k'_2 = 2k_2$ and $k''_2 = k_2/2$.

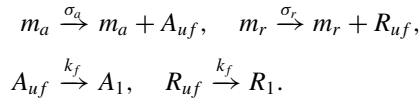
The mRNA transcription reactions are



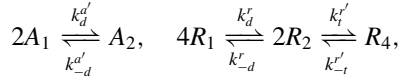
where $m_{a/r}$ represents the number of mRNA molecules of *araC/lacI* genes. When the promoter is not bound to either regulator, neither A_2 nor R_4 , it attains the state $P_{0,0}^{a/r}$ and the

mRNA transcription of the activator and repressor ($m_{a/r}$) proceeds at a basal rate b_a . The promoter bound to the AraC dimer is denoted by the state $P_{1,0}^{a/r}$, and results in the transcription induction rate by increasing transcription by a factor of α greater than the basal rate. There is a complete absence of transcription, when the promoter is bound by either one or two *lacI* tetramers, i.e., the promoter is in either the $P_{i,1}^{a/r}$ or $P_{i,2}^{a/r}$ state, respectively. Given that promoter looping by protein-DNA binding during LacI-induced repression is rapid, we have assumed that that looped DNA is in equilibrium with the state prior to looping. This simplification allows us to reduce the number of promoter states, as compared to the original model by Stricker *et al.* [15].

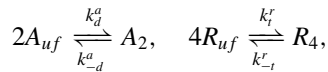
The resulting reactions representing mRNA translation and protein folding are



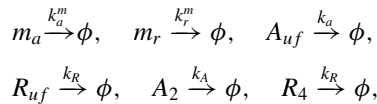
A_{uf} and R_{uf} are the unfolded activator and repressor proteins while A_1 and R_1 are the respective monomers, while $\sigma_{a/r}$ is the RBS efficiency of the activator/repressor and k_f is the folding rate of the proteins. These proteins are, however, transcriptionally active only in the form of dimers and tetramers, which involve the following reactions,



where A_2 is the dimeric AraC protein and R_2 and R_4 are the di- and tetrameric forms of the repressor protein. Based on the high forward rates of dimer (R_2) formation reported by Stricker *et al.* [15], we ignore the repressor dimer intermediates. Additionally, given that the activator dimer and repressor tetramer forward rates are two orders of magnitude faster as compared to the backward rates, i.e., $k_d^a \gg k_{-d}^a$ and $k_t^r \gg k_{-t}^r$, respectively [15], we simplify the protein production as



where the prefactors account for monomer equivalents of the multimers and k_d^a and k_{-d}^a and k_t^r and k_{-t}^r are the effective forward and backward rates of the activator dimer and repressor tetramer formation, respectively. Degradation reactions of mRNA and proteins are given by



where $k_{a/r}^m$ represents the respective mRNA degradation rates and $k_{A/R}$ of the respective proteins. This set of chemical mass-balance relations allows us to put together a combination of constitutive relations and differential equations to describe the oscillator dynamics.

At the level of DNA, the promoters of the activator and repressor ($P^{a/r}$) can be found in one of six states. The state not bound by any protein is $P_{0,0}$ and we assume promoter states

bound to proteins are at equilibrium, based on similar approximations made in gene-expression models previously [16,19], based on measured reaction rates. The remaining promoter states related to their equilibrium rate constants then are

$$P_{1,0} = k_1 A_2 P_{0,0}, \quad P_{0,1} = 2k_2 R_4 P_{0,0},$$

$$P_{0,2} = \frac{k_2}{2} R_4 P_{0,1} = \frac{k_2}{2} R_4 (2k_2 R_4 P_{0,0}) = k_2^2 R_4^2 P_{0,0},$$

$$P_{1,1} = (k_1 A_2) P_{0,1} = 2k_1 A_2 k_2 R_4 P_{0,0},$$

$$P_{1,2} = (k_1 A_2) P_{0,2} = k_1 A_2 k_2^2 R_4^2 P_{0,0}, \quad (1)$$

based on the mass balance of promoters with A_2 and R_4 . However, since the plasmid copy number n is constant for a given scenario, the total number of all promoter states is also constant, allowing us to impose a conservation condition,

$$n = \sum_{i,j} P_{i,j} = P_{0,0} + k_2 R_4 P_{0,0} + (k_2 R_4)^2 P_{0,0} + k_1 A_2 P_{0,0}$$

$$+ (k_1 A_2)(2k_2 R_4) P_{0,0} + (k_1 A_2)(k_2 R_4)^2 P_{0,0}$$

$$= [1 + k_1 A_2][1 + 2k_2 R_4 + (k_2 R_4)^2] P_{0,0}$$

$$= [1 + k_1 A_2][1 + k_2 R_4]^2 P_{0,0}. \quad (2)$$

Therefore, we describe the dynamics of the system in terms of mRNA and proteins. The production of mRNA of the activator (m_a) and repressor (m_r) are described, as in previous work, by the differential equations

$$\frac{dm_a}{dt} = n_a b (P_{0,0}^a + \alpha P_{1,0}^a) - k_a^m m_a,$$

$$\frac{dm_r}{dt} = n_r b (P_{0,0}^r + \alpha P_{1,0}^r) - k_r^m m_r. \quad (3)$$

Since we assume the promoter states are in equilibrium, we can rewrite $P_{1,0}$ in terms of $P_{0,0}$ using Eq. (1), and then $P_{0,0}$ in terms of n [Eq. (2)]. Substituting these values in Eq. (3), the mRNA dynamics are then represented by the following differential equations,

$$\frac{dm_a}{dt} = n_a \frac{b(1 + \alpha k_1 A_2)}{(1 + k_1 A_2)(1 + k_2 R_4)^2} - k_a^m m_a,$$

$$\frac{dm_r}{dt} = n_r \frac{b(1 + \alpha k_1 A_2)}{(1 + k_1 A_2)(1 + k_2 R_4)^2} - k_r^m m_r. \quad (4)$$

The translation of mRNA results in the production of nascent unfolded proteins, the dynamics of which can be described by

$$\frac{dA_{uf}}{dt} = \sigma_a m_a - k_f A_{uf} - k_A A_{uf},$$

$$\frac{dR_{uf}}{dt} = \sigma_r m_r - k_f R_{uf} - k_R R_{uf}. \quad (5)$$

In both these equations, the first term represents production by translation, while the second and third terms represent depletion of proteins due to folding and degradation, respectively. Unfolded proteins form monomers (A_1 and R_1) in a manner

TABLE I. The values of parameters used in the model are based on either previous reports [15], or are varied.

Parameter	Value	Description	Reference
b	0.36 min^{-1}	Basal transcription rate	[15]
α	20	Transcription activation	[15]
n_a	50	<i>araC</i> DNA copy number	[15]
n_r	25 and varied	<i>lacI</i> DNA copy number	[15] and this study
k_m^a	0.54 min^{-1}	Degradation rate of <i>araC</i> mRNA	[15]
k_m^r	0.54 min^{-1} and varied	Degradation rate of <i>lacI</i> mRNA	[15] and this study
σ_A	90 min^{-1}	RBS efficiency of <i>araC</i>	[15]
σ_R	90 min^{-1} and varied	RBS efficiency of <i>lacI</i>	[15] and this study
k_f	0.9 min^{-1}	Rate of folding of proteins	[15]
γ_0	1080 min^{-1}	Maximal degradation	[15]

dependent on the rate of protein folding (k_f), while the active forms of the proteins are dimers of the activator (A_2) and tetramers of the repressor (R_4). The total folded activator (A_t) and repressor (R_t) can be written as

$$\frac{dA_t}{dt} = k_f A_{uf} - k_A A_t, \quad \frac{dR_t}{dt} = k_f R_{uf} - k_R R_t, \quad (6)$$

where $A_t = A_1 + 2A_2$ and $R_t = R_1 + 2R_2 + 4R_4$ and R_2 represents the dimeric form of the repressor. We assume protein multimerization is at equilibrium. Monomers of the activator and repressor as well as repressor dimers are negligible at equilibrium, and the activator is expected to be largely found in the form of dimers (A_2) and the repressor in the tetrameric form (R_4).

This results from the two orders of magnitude faster forward rates of dimer/tetramer formation as compared to the backward rate, i.e., for the activator $k_d^a \gg k_{-d}^a$ and for the repressor, $k_d^r \gg k_{-d}^r$ and $k_t^r \gg k_{-t}^r$, based on a previous report by Stricker *et al.* [15]. Thus, our equilibrium assumption allows us to avoid the addition of a differential equation to explicitly model the dynamics of dimer and tetramer formation involving higher-order terms, as described previously [20]. The total proteins then are approximated by $A_t \approx 2A_2$ for the activator and $R_t \approx 4R_4$ for repressor proteins, which allows us to write the equilibrium concentrations of activator dimers and repressor tetramers as fractions of total protein concentration as follows,

$$A_2 = A_t/2, \quad R_4 = R_t/4. \quad (7)$$

The fractional terms are due to the stoichiometry of monomers. Their dynamics are then defined by substituting Eq. (7) in Eq. (6), resulting in the following differential equations,

$$\begin{aligned} \frac{dA_2}{dt} &= (1/2)k_f A_{uf} - k_R A_2, \\ \frac{dR_4}{dt} &= (1/4)k_f R_{uf} - k_R R_4. \end{aligned} \quad (8)$$

To account for the time taken by the proteins to fold and multimerize, we assume two time delays until equilibrium is achieved: τ_1 for the activator dimer (A_2) and τ_2 for the repressor tetramer (R_4) formation. These delays are relative to the rate of the rest of the reactions in the network. Additionally, based on the reported equality of the activator dimerization

and repressor tetramerization rates, i.e., $k_d^a = k_t^r$ (Table I), and the twofold difference in multimer size between dimers and tetramers, we consider the delay for tetramer formation to be twice that of the delay in the dimer, i.e., $\tau_2 = 2\tau_1$. This is akin to an approach used recently to model the dual-negative ara/lac oscillator [21]. The equality assumed between dimer and tetramerization rates respectively of the activator and repressor, based on Stricker *et al.*, could be tested in the future.

Thus, the delay considered in our equations represents the time taken for A_2 and R_4 to reach equilibrium, which we use as a term to determine mRNA production. We combine these simplifications together to arrive at a minimal model that includes regulation of mRNA transcription, protein translation and folding, and multimerization that feeds back to transcription.

B. Model description

Transcription is modeled in terms of the dynamics of two mRNA species, encoding the *araC* activator (m_a) and *lacI* repressor (m_r) and regulated by the feedback from the activator protein dimers and repressor protein tetramers. For simplicity, the protein complexes are referred to as A in place of A_2 and R in place of R_4 . The general equation of mRNA copies (m_x) for the activator ($x = a$) and repressor ($x = r$) is

$$\dot{m}_x = \frac{n_x b (1 + \alpha k_1 A(\tau_1))}{[1 + k_1 A(\tau_1)][1 + k_2 R(\tau_2)]^2} - k_m^x m_x, \quad (9)$$

where

$$x \in \{a, r\}.$$

The two parts of the right-hand side of the equation represent the production and degradation terms. The delay terms τ_1 and τ_2 are introduced to account for the time taken for monomeric proteins (A_1 and R_1) to fold and form dimers and tetramers at equilibrium, respectively. By assuming A and R are in equilibrium with their monomers, we achieve a simplification of the model. The terms $A(\tau_1) \equiv A(t - \tau_1)$ and $R(\tau_2) \equiv R(t - \tau_2)$ represent the equivalence of the number of protein multimers, where t is current time. The copy numbers of the genes encoding *araC* and *lacI*, n_a and n_r , respectively,

act as multiplication factors. Based on the reported copy number differences of the genes in the original experiment by Stricker *et al.* [15], we initially assume an asymmetry in the plasmid copy numbers, i.e., $n_a \neq n_r$. The transcription rate is determined by the basal transcription rate b , in the absence of an activator or repressor binding to the promoter. The multiplicative increase in transcription rate when the activator (A) is bound is given by α and the degradation rates of the activator and repressor mRNA are k_m^a and k_m^r , respectively. The terms k_1 and k_2 represent the equilibrium binding constants of A_2 and R_4 to the promoter, respectively, for a given inducer concentration, i.e., arabinose and IPTG. In contrast to the previous work [15], we considering the binding and unbinding of the activator and repressor to the promoter to be at equilibrium.

The equilibrium binding constant of AraC binding to the promoter is by k_1 , which depends on the concentrations of the inducers arabinose (ara) and IPTG as

$$k_1 = k_1^{\min} + (k_1^{\max} - k_1^{\min}) \frac{[ara]^2}{(\mu^2 + [ara]^2)} \frac{\nu^2}{(\nu^2 + [IPTG]^2)}. \quad (10)$$

The range of activator binding to the promoter is set by $k_1^{\min} = 0$ molecules⁻¹, $k_1^{\max} = 1$ molecules⁻¹, and $\mu = 2.5\%$ [in weight/volume percent (w/v%)] and $\nu = 1.8$ mM are scaling parameters, as before [15]. The *lacI*-promoter binding is determined by k_2 as follows,

$$k_2 = k_2^{\min} + (k_2^{\max} - k_2^{\min}) \frac{\lambda^2}{\lambda^2 + [IPTG]^2}, \quad (11)$$

where the repressor binding range is determined by $k_2^{\min} = 0.01$ molecules⁻¹, $k_2^{\max} = 0.2$ molecules⁻¹, and $\lambda = 0.035$ mM is a scaling parameter. We model gene-expression induction resulting from the presence of the sugars (arabinose and IPTG) that bind the activator and repressor proteins with a second-order dependence of both k_1 and k_2 on $[ara]$, $[IPTG]$, μ , ν , and λ to represent cooperativity of the reaction.

The mRNAs are translated into unfolded proteins A_{uf} and R_{uf} , the monomeric activator and repressor, respectively. The dynamics of translation of the unfolded protein species (X_{uf}) is given by the general expression

$$\dot{X}_{uf} = \sigma_x m_x - k_f X_{uf} - k_x X_{uf}, \quad (12)$$

where

$$X \in \{A, R\}, \quad \text{and } x \in \{a, r\},$$

where σ_x is the translation rate of x that corresponds to A_{uf} and R_{uf} . This is also referred to as the ribosome binding site (RBS) efficiency in the synthetic biology literature [22]. The folding rate k_f is constant and common to both proteins, while the degradation rate of the unfolded protein k_x is variable due the *srA* tag that results in rapid degradation [15] by proteolysis mediated by ClpXp [23]. To account for the fact that the number of ClpXp molecules available to degrade proteins is limiting, the degradation rate for repressor is given as

$$k_R = \frac{\gamma_0}{c_0 + \Sigma P}, \quad (13)$$

while that for the activator is given as

$$k_A = \chi k_R. \quad (14)$$

Here, γ_0 is the maximal degradation rate, $c_0 = 0.1$ is the concentration of proteins at which the rate of ClpXp is half maximal, and $\chi = 2.5$ represents the differential degradation of two proteins, i.e., the activator is degraded faster than the repressor. The total copy number of all proteins in this system thus inversely determines the degradation rate. The total proteins are $\Sigma P = A_{uf} + R_{uf} + A_t + R_t$, based on the equilibrium assumption summarized in Eq. (7), based on which we simplify the model and exclude the dynamics of the folded monomers A_t and R_t [Eq. (5)].

Based on the equilibrium assumption, the dynamics of the activator dimers (A) and repressor tetramers (R) can therefore be generalized from Eq. (8) as

$$\dot{X} = \frac{1}{p_X} k_f X_{uf} - k_X X. \quad (15)$$

where

$$X \in \{A, R\},$$

where k_f is the folding rate, X_{uf} represents the unfolded protein, and the proportionality constants $p_A = 2$ and $p_R = 4$ account for the dimerization and tetramerization of the activator and repressor, respectively [Eqs. (7) and (8)]. As a consequence, at any time point, the dimers are half ($1/p_A$) the number of monomers, and tetramers are 1/4th ($1/p_R$) the number of monomers at the same time.

The simplifications resulting from the assumed equilibrium in protein folding, dimerization, and tetramerization as well as promoter binding are accounted for in our equations by explicit delays. Such an approach of using delays to account for intermediate processes (typically transcription) without explicitly modeling them has been used successfully used to model negative-feedback oscillators [24] and the *lac* operon [25].

This allows us to arrive at six equations [Eqs. (9), (12), and (15) for the activator and repressor] that fully describe the system.

III. RESULTS

A. Minimal model with parametrized delay, reproducing experimental oscillatory dynamics

The model parameters are taken from previous reports (Table I), leaving two free parameters, the delay terms τ_1 and τ_2 for the activator and repressor, respectively. We factorize the delay to only one free parameter, since $\tau_2 = 2\tau_1$ as discussed in the section entitled ‘‘Model derivation.’’ The one free parameter τ_1 is estimated to be of the order of minutes and numerically estimated by simulating for a range of values of τ_1 (0–5 min in 0.25-min intervals) using the period of oscillations as a measure to compare the deviation between simulation and experiment [15] with inducers $[IPTG] = 2$ mM and 0.7% arabinose. We find τ_1 of 1.25 min to be optimal, since it minimizes the difference between the simulation and experiment and results in sustained oscillations of *araC* and *lacI* at the level of both mRNA and protein complexes [Fig. 2(a)]. Our simulations result in the same period and amplitude to those reported by solving the detailed model described by Stricker *et al.* [15].

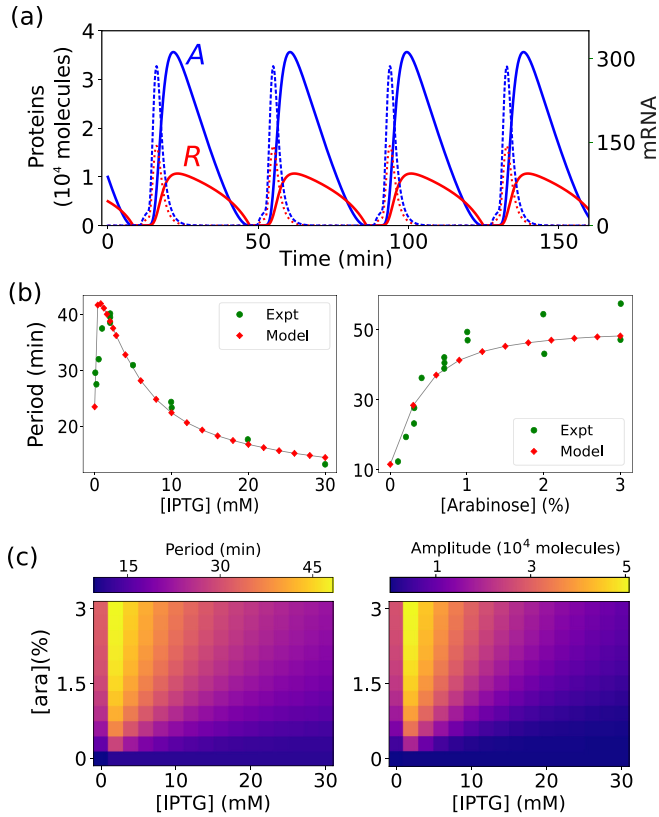


FIG. 2. (a) The number of molecules of *araC* mRNA (dotted blue/dark-gray line) and protein dimers (solid blue/dark-gray line) and *lacI* mRNA (dotted red/light-gray line) and protein tetramers (solid red/light-gray line) are plotted as a function of time for the minimal model. Here, $n_a = 50$, $n_r = 25$, $[\text{ara}] = 0.7\%$, and $[\text{IPTG}] = 2$ mM. (b) The period of oscillations predicted by the model (\blacklozenge) is compared to experimental data from Stricker *et al.* [15] (\bullet) for increasing inducer concentrations of (left) IPTG ($[\text{arabinose}] = 0.7\%$) and (right) arabinose ($[\text{IPTG}] = 2$ mM). (c) The phase diagram plots the effect of a systematic change in IPTG and arabinose concentrations on the oscillatory (left) period and (right) amplitude. Color/gray bars represent the respective scales.

The so-called “degrade-and-fire” (DF) behavior of the oscillator observed [24] is consistent with the mechanism of a basal mRNA transcription rate (b) producing low concentrations of protein, that are constantly degraded by proteolysis, determined by γ_0 and c_0 . Since the production of AraC dimers is faster than the LacI tetramers, the activator protein induces network expression, initially at a slow rate, and then at increasing rates via the positive-feedback loop (“fire”). The repressor protein concentration is, however, also gradually increasing, and once it reaches a threshold required for promoter repression, the negative-feedback loop begins to inhibit transcription. This negative feedback reduces mRNA levels, and combined with the mRNA degradation rates k_m^a and k_m^r , turns the network off (“degrade”). The basal transcription rate then once more induces the cycle, resulting in oscillations.

In addition, the time period of oscillations responds differently to increasing concentrations of IPTG as compared to arabinose, consistent with experimental reports [Fig. 2(b)]. While increasing the IPTG concentration up to 1 mM

increases the period, higher values decrease the period (while arabinose is held constant at 0.7%), as a result of the inhibitory effect of high concentrations of IPTG on *araC* binding to the promoter [Eq. (10)], based on previous reports. On the other hand, increasing arabinose concentrations from 0% to 3% with constant IPTG (2 mM) results in saturation-type behavior of the oscillatory period [Fig. 2(b)]. The agreement between our reduced model and previously reported experimentally determined values [15], both in terms of the period and amplitude of oscillations [Fig. 2(c)], suggests that it successfully captures the essential dynamics of the system, despite the multiple simplifying assumptions.

Since the model developed previously by Stricker *et al.* [15] required an asymmetry in activator and repressor molecules to produce oscillations, we proceeded to test the sensitivity of the model to both the extent of asymmetry and whether DNA asymmetry can be mimicked by translational asymmetry.

B. Effect of gene copy number asymmetry on oscillations

In previous experimental and theoretical work where the *lac-ara* oscillator was first developed [15], the genes encoding the activator and repressor were expressed from two different plasmids that were maintained in cells at different copy numbers. The gene copy number of DNA molecules encoding the activator was 50 and the repressor was 25, a ratio of $n_a : n_r = 2 : 1$. Our model uses the same values in order to reproduce experimental data (Fig. 2). However, both cell to cell variability due to molecular states, as well the differences in the stage of division, could result in variations in plasmid copy numbers. Additionally, the cell-cell variability in the plasmid copy number due to the imprecision or “noise” in the copy number control of the plasmids cannot be ruled out. To investigate this, we have examined the effect of varying the asymmetry of the DNA copies of the activator (n_a) and repressor (n_r) on the oscillatory dynamics. We find that when the activator gene copies are twofold in excess of or equal to those of the repressor, the oscillations are rapid and the amplitudes comparable. However, a twofold excess of repressor copies results in a small increase in the period of oscillation of both the activator protein A [Fig. 3(a)] and repressor R [Fig. 3(b)]. Indeed, the copy number asymmetry, $\rho_C = (n_a - n_r)/(n_a + n_r)$, appears to drive the increased amplitude of that gene, i.e., if the asymmetry involves an excess of *lacI* DNA copy numbers, then a higher amplitude of the corresponding repressor protein R as compared to the activator A is observed, and vice versa.

A systematic scan across ρ_C ranging from -0.4 to 0.4 (repressor DNA in excess to activator DNA in excess) demonstrates a continuous decrease in period, i.e., increase in oscillation frequency [Fig. 3(c)], while the repressor amplitude reduces and the activator amplitude increases [Fig. 3(d)]. This would suggest that at some higher factor of asymmetry ($\rho_C < -0.4$), the oscillator period would become very large and not allow for “rapid” oscillations, within a generation of the bacterium (~ 50 min [26]). Indeed, it suggests that a DNA copy number asymmetry ensures fast oscillations.

Based on these results, we proceed to explore the redesign of the circuit by assuming that both genes are on the same

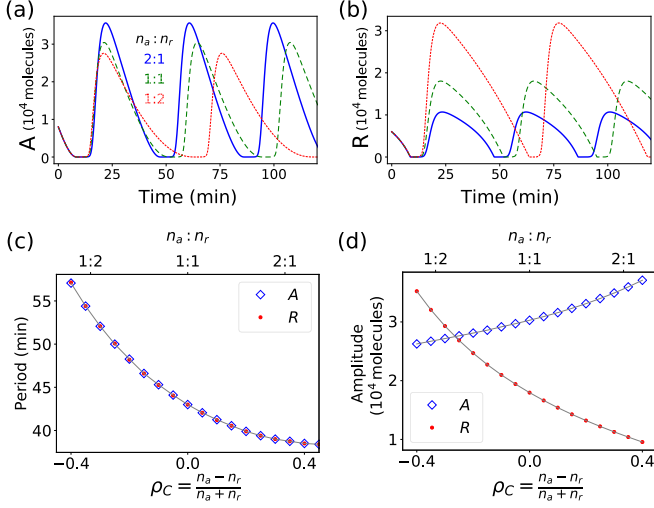


FIG. 3. Effect of relative DNA copy number asymmetry on oscillations. (a), (b) The effect of the gene copy number ratio of the activator n_a (*araC*) and repressor n_r (*lacI*) on the (a) activator dimer and (b) repressor tetramer concentration is plotted as a function of time. Individual plots signify $n_a : n_r$ 2:1 (solid), 1:1 (dashed), and 1:2 (dotted). (c), (d) The effects of the copy number asymmetry (ρ_C) and ratio $n_a : n_r$ on (c) the oscillatory period and (d) amplitude of the activator (\diamond) and repressor (\bullet) are plotted. [IPTG] = 2 mM, [Arabinose] = 0.7%, $n_a = 50$, and $n_r = 19$ –150.

plasmid (i.e., $n_a = n_r$), with the aim of minimizing cell-cell variability in oscillatory behavior due to plasmid DNA copy number variability. However, given our result demonstrating the need for asymmetry in gene copy numbers to ensure rapid oscillations, we proceeded to ask if the asymmetry of mRNA translation could replace the asymmetry in the DNA copy number.

C. DNA copy number and RBS efficiency have an equivalent effect on protein oscillations

We aimed to address the question of whether a symmetric DNA copy number ratio (ρ_C) can be replaced with an equivalent mRNA translation asymmetry. In order to achieve this, we tested whether the asymmetry in the ribosome binding site (RBS) affinity $\rho_R = (\sigma_a - \sigma_r)/(\sigma_a + \sigma_r)$ could achieve the same effect. This is also motivated by quantitative evidence of the tunability of protein translation through RBS modulation [22]. We therefore attempted to derive an expression for protein translation in terms of the transcription and translation terms. We start from the transcription rate equation for the mRNA production of the activator (m_a) and repressor (m_r) expressed in terms of the general equation for m_x as

$$\dot{m}_x = n_x g(A_{\tau_1}, R_{\tau_2}) - k_m^x m_x, \quad x \in \{a, r\}, \quad (16)$$

where $g(A_{\tau_1}, R_{\tau_2})$ is the nonlinear term in Eq. (9) and k_m^x stands for the degradation rates k_m^a and k_m^r of the activator and repressor, respectively. We now use the integrating factor method to write the functional form of the solution,

$$m_x = e^{-k_m^x t} \int n_x g(A_{\tau_1}, R_{\tau_2}) e^{k_m^x t} dt. \quad (17)$$

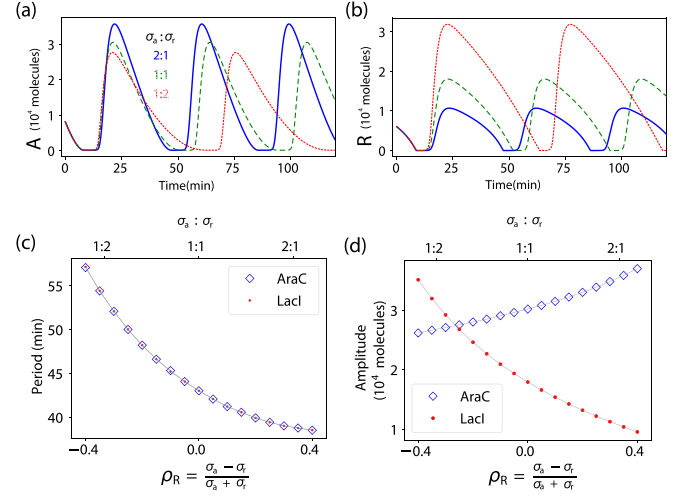


FIG. 4. Simulations of RBS efficiency asymmetry. Oscillations in the concentration of (a) AraC dimers and (b) LacI tetramers are obtained even when the copy number ratio ($n_a : n_r$) is kept fixed at 1:1 and the RBS efficiency ratio ($\sigma_a : \sigma_r$) is varied; simulations were run for constant IPTG and arabinose input of 2 mM and 0.7%, respectively. For the same IPTG and arabinose concentration, the dependence of (c) time period and (d) amplitude on the copy number ratio is shown. It can be seen that this produces exactly the same effect as keeping the RBS efficiency constant and changing the copy number.

Substituting this in the protein translation equation that results in an unfolded protein (X_{uf}) from mRNA [Eq. (5)], we obtain

$$\dot{X}_{uf} = \sigma_x \left(e^{-k_m^x t} \int n_x g(A_{\tau_1}, R_{\tau_2}) e^{k_m^x t} dt \right) - k_f X_{uf} - k_X X_{uf}. \quad (18)$$

Since n_x is a constant, it is taken out of the integration, resulting in the expression for the rate of unfolded protein formation,

$$\dot{X}_{uf} = (\sigma_x n_x) \left(e^{-k_m^x t} \int g(A_{\tau_1}, R_{\tau_2}) e^{k_m^x t} dt \right) - k_f X_{uf} - k_X X_{uf}. \quad (19)$$

This expression has a multiplicative factor consisting of two constants n_x and σ_x , demonstrating the exact equivalence of the DNA copy number and RBS efficiency. This is also confirmed by numerical simulation (Fig. 4).

Thus, we can demonstrate that transcriptional asymmetry can be replaced by translational asymmetry, while reproducing the oscillatory dynamics reported before. However, one of the goals of redesigning the network based on the principles of gene transcription and translation also involves expanding the tunability range of the system. With this in mind, we proceeded to test the role of degradation rates on the oscillator.

D. Expanding the tunability of the oscillator based on mRNA degradation rate asymmetry

Since the production of RNA functions as a simple multiplicative factor of the DNA copy number, in the search for additional levels to modify the tunability of the network, we

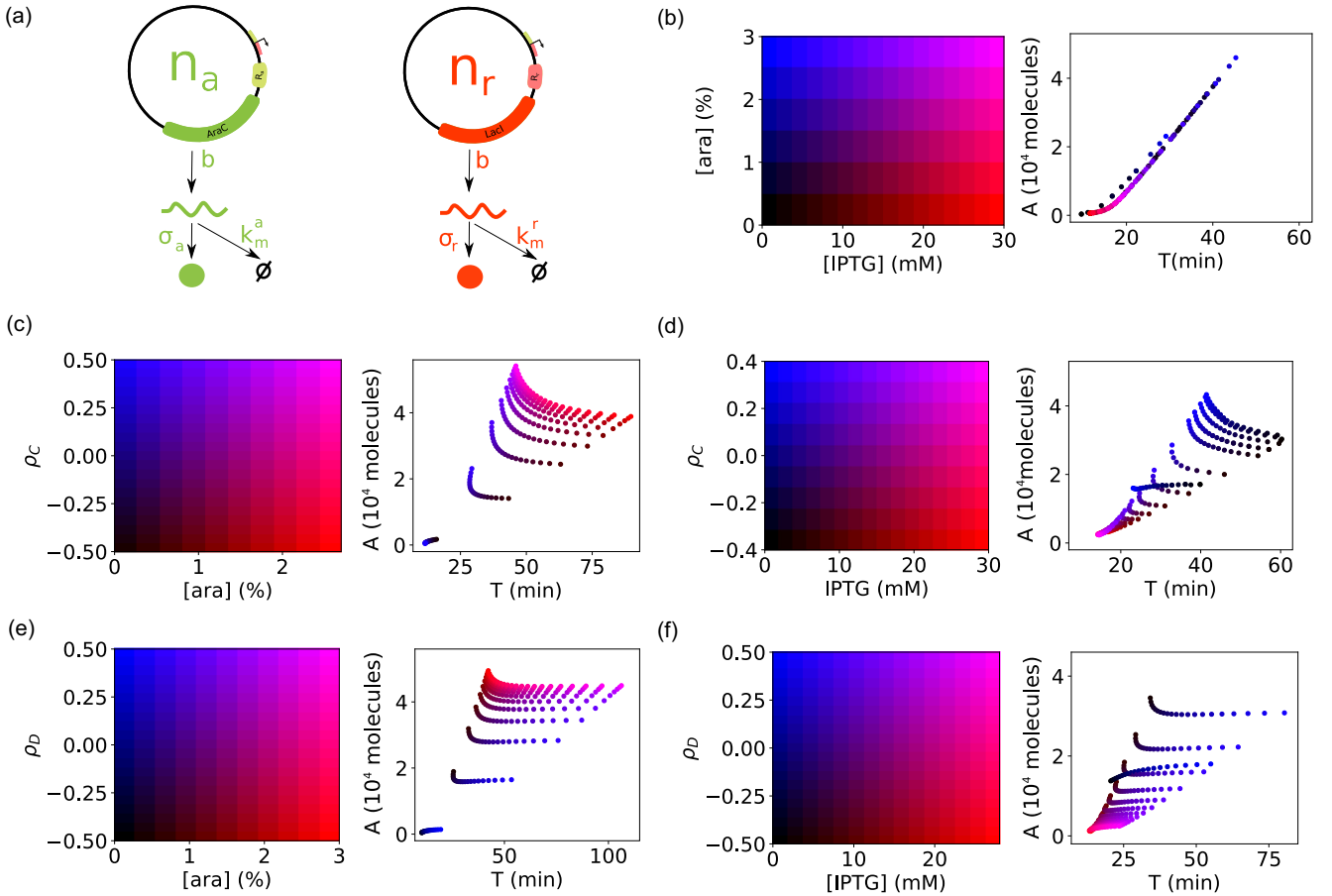


FIG. 5. Network tunability of the oscillator with asymmetry in the gene copies and mRNA degradation. (a) The schematic represents the asymmetry of the activator and repressor that we test in terms of the copy numbers n_a and n_r (ρ_C), and the mRNA degradation rates k_a and k_r (ρ_D), respectively, while σ_a/r represent the respective rate of mRNA translation to unfolded proteins. (b)–(f) The tunability of the oscillator measured by the amplitude (A) in 10^4 molecules plotted against the period (T) in minutes. (b) The effect of varying concentration of the inducers IPTG and arabinose (color/gray matrix) for a constant DNA copy number asymmetry of $\rho_C = 0.33$ ($n_a = 50$, $n_r = 25$) seen in experiment results in points that overlap one another, while (c) and (d) modifying ρ_C together with either increasing (c) arabinose for a constant [IPTG] = 2 mM or (d) IPTG for a constant [arabinose] = 0.7% results in a wider range of A and T . (e), (f) A similar scan of parameters is performed for ρ_D changes in response to increasing (e) [IPTG] or (f) [arabinose]. The colors in the plots indicate parameter value inputs: [IPTG] = 0–30 mM in steps of 2 mM, [arabinose] = 0%–3% in steps of 0.3%, (3) ρ_C and $\rho_D = -0.5$ to $+0.5$ in steps of 0.05 (please refer to the online figure for more details).

tested whether the degradation rate would potentially affect the dynamics any differently. This is motivated in part by the development of experimental tools that allow mRNA degradation rate control [27,28], and the reported role of mRNA degradation rates in modulating mean expression levels [28]. The degradation rate asymmetry $\rho_D = (k_m^a - k_m^r)/(k_m^a + k_m^r)$ is therefore compared to the DNA copy number asymmetry for the effect on oscillations [Fig. 5(a)].

In experiments by Stricker *et al.* [15], the gene (i.e., DNA) copy numbers of the activator (n_a) were 50 and those of the repressor (n_r) 25. When we simulated oscillations with this copy number asymmetry, $\rho_C = (n_a^a - n_r^r)/(n_a^a + n_r^r)$ of 0.33, we found increasing IPTG concentration resulted in an almost linear decrease in the period of oscillations (higher frequency) and amplitude, while increasing the arabinose concentration resulted in proportionately increasing the period and amplitude [Fig. 5(b)]. Changing both IPTG and arabinose simultaneously (diagonal along the color map of inducers) results in an intermediate value of period and amplitude that

follows the same trend. This suggests that for a given DNA copy number asymmetry, the oscillatory period and amplitude are coupled. Thus, when the plasmid DNA copy number asymmetry $\rho_C = (n_a - n_r)/(n_a + n_r)$ was varied, the amplitude and period of oscillations resulted in a widened “fan” for higher concentrations of both arabinose [Fig. 5(c)] and IPTG [Fig. 5(d)]. This suggests that copy number asymmetry can be used to modulate the oscillator, so it explores a wider range of amplitude and period. In experimental terms, the likely scenario is, however, that a given ρ_C is used, due to the nature of the plasmids. In such a case, the system responds to inducer titration with linear increases in both period as well as amplitude. On the other hand, with an mRNA degradation rate asymmetry $\rho_D = (k_m^a - k_m^r)/(k_m^a + k_m^r)$ with less stable repressor mRNA, varying arabinose [Fig. 5(e)] and IPTG [Fig. 5(f)] demonstrates a large change in amplitude, for a relatively narrow period (20–40 min). This is only seen when the degradation rate asymmetry $\rho_D < 0$, indicative of a faster degradation of the repressor mRNA. At higher ρ_D values

the oscillator appears to respond to inducer concentrations, similarly to the effect of ρ_C .

This suggests that engineering a system with the activator and repressor genes on the same plasmid, and with faster degradation rates for the repressor (i.e., $k_m^r > k_m^a$), could allow independent tunability of the period and amplitude. This would appear to suggest that while the experimental system based on two plasmids can produce fast, tunable oscillations in proteins, their robustness to cell to cell variability can be improved by expressing the proteins at the same level (symmetric RBS efficiency) and including an asymmetry in the degradation rates of mRNAs.

IV. DISCUSSION

We have successfully developed a minimal model of the dual-feedback loop tunable genetic oscillator, which still maintains sufficient detail to explore the regulation of the system at the levels of the canonical central dogma—DNA, RNA, and protein. We have optimized a single free parameter, the delay term to obtain oscillatory dynamics that match the whole range of experimental values. Using this minimal model, we explore the role of asymmetry of the activator and repressor, in terms of DNA copy numbers and the production and degradation rates of mRNA. We find that while rapid oscillations can be produced when a twofold excess of activator genes is present, this asymmetry is mathematically identical to mRNA production rates. On the other hand, mRNA degradation rate asymmetry results in a wider tunability of the oscillator. Thus, with this simplified model of a canonical synthetic genetic oscillator, we predict a more robust design of the oscillator, capable of exploring a wider range of frequency and amplitudes.

While attempts to simplifying the lac-ara dual-feedback oscillator have been made, they have ignored the role of mRNA, modeling only the DNA and protein components [21,29]. As a result, the ability to explore novel network design is limited. In their work, multiple parameters are fit to experimental data, which could result in artifacts. In our work, we have maintained identical parameters to the published model and experimental work of Stricker *et al.* [15], as well as used experimentally tested ranges of inducers (IPTG and arabinose), while leaving only one free parameter, the delay term. We have thus developed a simplification of this model oscillatory network.

A redesign of the dual-feedback oscillators has been recently proposed in terms of a new activator for the protease that degrades the proteins [29]. Our findings of copy number, translational efficiency, and mRNA degradation rate asymmetry suggest we can achieve semi-independent independent tunability of the amplitude and time period by changing the IPTG or arabinose concentrations. This approach is naturally also simpler in design and potentially easier to implement experimentally.

While we have explored the role of asymmetry in oscillatory dynamics, it is clear from our simulations that the copy number and translation symmetry can also result in oscillations. This is consistent with the results of a model of where a dual-feedback oscillator with symmetric components can still oscillate as described by Maeda *et al.* [14]. In addition, while the protein oscillations of asymmetry in copy number

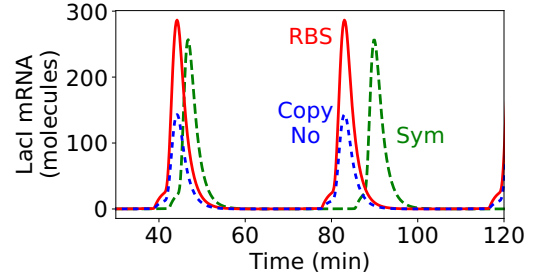


FIG. 6. The dynamics of *lacI* transcripts for symmetric and asymmetric models. The dynamics of *lacI* mRNA are plotted for (i) an asymmetric DNA copy number ratio $n_a : n_r = 2 : 1$ (dashed line, closely spaced), (ii) RBS asymmetry of $\sigma_a : \sigma_r = 2 : 1$ (solid line), and (iii) symmetric copy number and RBS efficiency $n_a : n_r = \sigma_a : \sigma_r = 1 : 1$ (dashed line, widely spaced).

(ρ_C) and RBS efficiency (ρ_R) are equivalent, the mRNA transcripts differ (Fig. 6). In addition, a comparison of genetic oscillator designs suggests that symmetric gene networks while used in models are unlikely to be natural [18]. Indeed, the assumption of many standard genetic oscillator models such as the “repressilator” model is that mRNA degradation rates are comparable for the component genes [12]. Indeed, recent work has demonstrated the possibility to achieve fine-tuned control over protein levels through mRNA degradation rate modulation, simply by varying the length of the polyA tail [30]. Here, by exploring the possible differences in copy numbers, RBS efficiency, and mRNA stability of the two-component network, we have explored more biologically realistic properties of networks, and find the effects of asymmetry depend on the level in the information flow at which they are implemented—DNA, RNA, or protein.

The role of stochasticity in genetic networks, especially when small numbers of proteins regulate the process, are known to be important. Indeed, based on previous work demonstrating the effect of stochasticity on this oscillatory system [15], we tested the effect of one source of experimental stochasticity, namely, the initial value of protein concentrations. We find the model oscillatory period and amplitude to be insensitive to fluctuations in the initial values (Fig. 7). The variability in the initial values is potentially likely due to potential asymmetry in the distribution of LacI and AraC proteins at division, as predicted for low copy number proteins [31]. A stochastic differential equation model of our reduced model could in the future help further explore alternative sources of variability that might originate from intrinsic cell-cell variabilities in proteins extrinsic to our model.

The role of the host cell machinery in determining the aspects of the genetic oscillator dynamics has been explored previously, showing that negative-feedback loop oscillators such as circadian oscillators can phase lock to the cell cycle [32], which natural oscillators avoid by using protein phosphorylation, asynchronous replication, and “noise” [33]. This would suggest the robustness of the *lac-ara* oscillator seen in experiments could be the combined result of the positive-feedback loop as well as the noise coming from replication asynchrony and copy number variability [15]. Experiments with the oscillator genes localized on the same plasmid, to

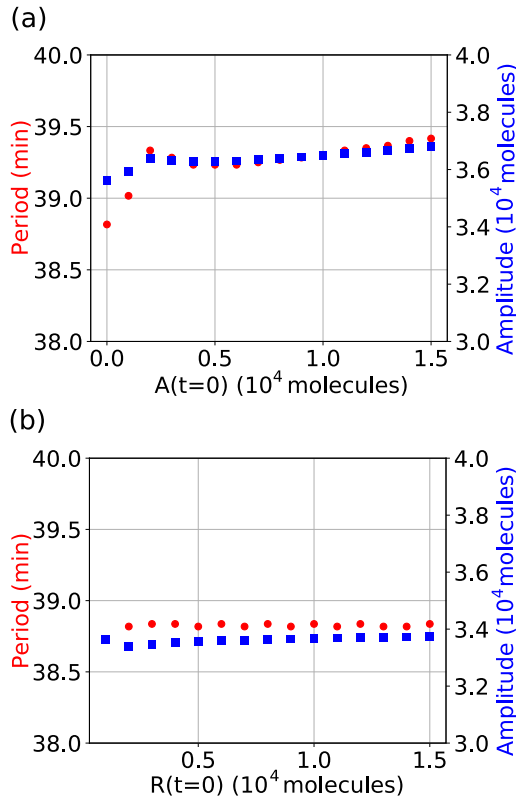


FIG. 7. Effect of initial values of the activator and repressor protein. The period (●) and amplitude (■) of the minimal oscillator model (based on delay differential equations) for varying initial concentrations, i.e., at $t = 0$, of the (a) activator (A) and (b) repressor (R) are plotted. Here, all other key parameters are kept constant: The ratio of plasmids $n_a : n_r$ is 2:1 (similar to the Stricker model) and the concentrations of the inducers are 2 mM IPTG and 0.7% arabinose with symmetric translation rates ($t_a : t_r = 1 : 1$).

separate the effects due to copy number variability and other sources of noise, could potentially answer some of these questions.

ACKNOWLEDGMENTS

We wish to acknowledge discussions with Dr. Pranay Goel regarding delay differential equations. Y.J.J. is supported by

a KVPY Scholarship No. SB-152085 from the Department of Science and Technology (DST), Government of India. Y.K.J. is supported by a project assistantship from Grant No. BT/PR16591/BID/7/673/2016 from the Department of Biotechnology, Government of India to CAA. The work began as a part of an iGEM2017 project and was supported through a one-time sponsorship by Lupin Pvt. Ltd., India.

APPENDIX: NUMERICAL SIMULATIONS AND ANALYSIS

In summary, we have reduced the mathematical model given by Ref. [15], with more than 30 equations, to a simplified model having only six differential equations, two of which are delay differential equations. We use two delay terms, τ_1 (activator) and τ_2 (repressor), and relate them as $\tau_2 = 2\tau_1$. This is based on the fact that activator proteins bind to DNA after dimerization, a one-step process, but the repressor binds after tetramerization, involving two intermediate steps. Since the rate constants for all these reactions have the same value according to previous reports [15], and promoter binding is much faster than multimerization, we argue that the delay due to two consecutive reactions is twice that of a single reaction. This model was simulated using PYTHON 3.6 and for the purpose of solving delay differential equations, the PyDDE package was used. To solve a delay differential equation numerically, the solver needs to be given initial data of all the variables between time $0 < t < 2\tau$. To get around this problem, we solve the equations as simple ODEs between $0 < t < 2\tau$ and as DDEs when $t > 2\tau$

A custom written peak-finding algorithm was used for estimation of the time period and amplitude. This algorithm involved comparing the concentration value at each time point with that of some time before and some time after the particular point. If $y(t)$ denotes the time series of protein concentrations, for any time t , we check if

$$y(t_0) > y(t_0 - s) \quad \text{and} \quad y(t_0) > y(t_0 + s). \quad (A1)$$

If the above condition is satisfied for all $s \in \{\delta t, 2\delta t, 30\delta t\}$, then we consider t_0 to be a “peak.” Our calculations were run with δt values of 0.2 min. The period and amplitude can be found by averaging the time difference between consecutive peaks and the values of $y(t_0)$, respectively.

[1] J. W. Newport and M. W. Kirschner, Regulation of the cell cycle during early xenopus development, *Cell* **37**, 731 (1984).
 [2] A. W. Murray and M. W. Kirschner, Dominoes and clocks: The union of two views of the cell cycle, *Science* **246**, 614 (1989).
 [3] B. Novak and J. J. Tyson, Numerical analysis of a comprehensive model of M-phase control in Xenopus oocyte extracts and intact embryos, *J. Cell. Sci.* **106**, 1153 (1993).
 [4] B. Novak and J. J. Tyson, Modeling the control of DNA replication in fission yeast, *Proc. Natl. Acad. Sci. USA* **94**, 9147 (1997).
 [5] J. E. Ferrell, Jr., T. Y.-C. Tsai, and Q. Yang, Modeling the cell cycle: Why do certain circuits oscillate?, *Cell* **144**, 874 (2011).
 [6] M. Ishiura, S. Kutsuna, S. Aoki, H. Iwasaki, C. R. Andersson, A. Tanabe, S. S. Golden, C. H. Johnson, and T. Kondo, Expression of a gene cluster kaiABC as a circadian feedback process in cyanobacteria, *Science* **281**, 1519 (1998).
 [7] J. Stelling, E. D. Gilles, and F. J. Doyle III, Robustness properties of circadian clock architectures, *Proc. Natl. Acad. Sci. USA* **101**, 13210 (2004).
 [8] K. Horikawa, K. Ishimatsu, E. Yoshimoto, S. Kondo, and H. Takeda, Noise-resistant and synchronized oscillation of the segmentation clock, *Nature (London)* **441**, 719 (2006).
 [9] J. Lewis and E. M. Ozbudak, Deciphering the somite segmentation clock: Beyond mutants and morphants, *Dev. Dyn.* **236**, 1410 (2007).

- [10] K. Uriu, Y. Morishita, and Y. Iwasa, Traveling wave formation in vertebrate segmentation, *J. Theor. Biol.* **257**, 385 (2009).
- [11] A. Becskei and L. Serrano, Engineering stability in gene networks by autoregulation, *Nature (London)* **405**, 590 (2000).
- [12] M. B. Elowitz and S. Leibler, A synthetic oscillatory network of transcriptional regulators, *Nature (London)* **403**, 335 (2000).
- [13] V. Noireaux, R. Bar-Ziv, and A. Libchaber, Principles of cell-free genetic circuit assembly, *Proc. Natl. Acad. Sci. USA* **100**, 12672 (2003).
- [14] K. Maeda and H. Kurata, A symmetric dual feedback system provides a robust and entrainable oscillator, *PLoS ONE* **7**, e30489 (2012).
- [15] J. Stricker, S. Cookson, M. R. Bennett, W. H. Mather, L. S. Tsimring, and J. Hasty, A fast, robust and tunable synthetic gene oscillator, *Nature (London)* **456**, 516 (2008).
- [16] J. Hasty, M. Dolnik, V. Rottschäfer, and J. J. Collins, Synthetic Gene Network for Entraining and Amplifying Cellular Oscillations, *Phys. Rev. Lett.* **88**, 148101 (2002).
- [17] N. Yildirim and M. C. Mackey, Feedback regulation in the lactose operon: A mathematical modeling study and comparison with experimental data, *Biophys. J.* **84**, 2841 (2003).
- [18] O. Purcell, N. J. Savery, C. S. Grierson, and M. Di Bernardo, A comparative analysis of synthetic genetic oscillators, *J. R. Soc. Interface* **7**, 1503 (2010).
- [19] J. Hasty, F. Isaacs, M. Dolnik, D. McMillen, and J. J. Collins, Designer gene networks: Towards fundamental cellular control, *Chaos* **11**, 207 (2001).
- [20] M. Santillán, On the use of the Hill functions in mathematical models of gene regulatory networks, *Math. Model. Nat. Phenom.* **3**, 85 (2008).
- [21] A. Veliz-Cuba, A. J. Hirning, A. A. Atanas, F. Hussain, F. Vancia, K. Josić, and M. R. Bennett, Sources of variability in a synthetic gene oscillator, *PLoS Comput. Biol.* **11**, e1004674 (2015).
- [22] A. Levin-Karp, U. Barenholz, T. Bareia, M. Dayagi, L. Zelcbuch, N. Antonovsky, E. Noor, and R. Milo, Quantifying translational coupling in E. coli synthetic operons using RBS modulation and fluorescent reporters, *ACS Synth. Biol.* **2**, 327 (2013).
- [23] N. A. Cookson, W. H. Mather, T. Danino, O. Mondragón-Palmino, R. J. Williams, L. S. Tsimring, and J. Hasty, Queuing up for enzymatic processing: Correlated signaling through coupled degradation, *Mol. Systems Biol.* **7**, 561 (2011).
- [24] W. Mather, M. R. Bennett, J. Hasty, and L. S. Tsimring, Delay-Induced Degrade-and-Fire Oscillations in Small Genetic Circuits, *Phys. Rev. Lett.* **102**, 068105 (2009).
- [25] N. Yildirim, M. Santillan, D. Horike, and M. C. Mackey, Dynamics and bistability in a reduced model of the lac operon, *Chaos* **14**, 279 (2004).
- [26] M. S. Gangan and C. A. Athale, Threshold effect of growth rate on population variability of escherichia coli cell lengths, *R. Soc. Open Sci.* **4**, 160417 (2017).
- [27] J. C. Liang, A. L. Chang, A. B. Kennedy, and C. D. Smolke, A high-throughput, quantitative cell-based screen for efficient tailoring of RNA device activity, *Nucleic Acids Res.* **40**, e154 (2012).
- [28] M. Mundt, A. Anders, S. M. Murray, and V. Sourjik, A system for gene expression noise control in yeast, *ACS Synth. Biol.* **7**, 2618 (2018).
- [29] M. Tomazou, M. Barahona, K. M. Polizzi, and G. B. Stan, Computational re-design of synthetic genetic oscillators for independent amplitude and frequency modulation, *Cell Syst.* **6**, 508 (2018).
- [30] L. L. Arthur, J. J. Chung, P. Jankirama, K. M. Keefer, I. Kolotilin, S. Pavlovic-Djuranovic, D. L. Chalker, V. Grbic, R. Green, R. Menassa, H. L. True, J. B. Skeath, and S. Djuranovic, Rapid generation of hypomorphic mutations, *Nat. Commun.* **8**, 14112 (2017).
- [31] N. Rosenfeld, J. W. Young, U. Alon, P. S. Swain, and M. B. Elowitz, Gene regulation at the single-cell level, *Science* **307**, 1962 (2005).
- [32] J. Paijmans, M. Bosman, P. R. Ten Wolde, and D. K. Lubensky, Discrete gene replication events drive coupling between the cell cycle and circadian clocks, *Proc. Natl. Acad. Sci. USA* **113**, 4063 (2016).
- [33] J. Paijmans, D. K. Lubensky, and P. Rein ten Wolde, Robustness of synthetic oscillators in growing and dividing cells, *Phys. Rev. E* **95**, 052403 (2017).